Proceedings of the 12th International Conference on Cosmic Rays, Hobart, 1971 (University of Tasmania, Tasmania, Australia, 1971), Vol. 1, p. 221.

[11]W. R. Webber, S. V. Damle, and J. Kish, Astrophys. Letters 9, 125 (1971).

[12]G. M. Mason, Astrophys. J. 171, 139 (1972).

[13]A. Buffington, L. H. Smith, G. Smoot, M. A. Wahlig, and L. W. Alvarez, in *Proceedings of the 12th International Conference on Cosmic Rays, Hobart, 1971* (see Ref. 10), Vol. 1, p. 146.

[14]J. F. Ormes, V. K. Balasubrakmanyan, and M. J. Ryan, in *Proceedings of the 12th International Conference on Cosmic Rays, Hobart, 1971* (see Ref. 10), Vol. 1, p. 178.

[15]G. Raisbeck and F. Yiou, Phys. Rev. Letters 27, 875 (1971).

[16]H. Reeves, W. A. Fowler, and F. Hoyle, Nature 226, 727 (1970).

[17]M. Meneguzzi, J. Audouze, and H. Reeves, Astron. and Astrophys. 15, 337 (1971).

[18]J. Radin, S. Korff, A. Smith, and N. Little, to be published; J. Radin, Ph.D. thesis, New York University, 1971 (unpublished).

[19]M. Jung, C. Jacquot, C. Baixeras-Aiguabella, R. Schmitt, and H. Braun, Phys. Rev. C 1, 435 (1970); M. Jung, C. Jacquot, C. Baixeras-Aiguabella, R. Schmitt, H. Braun, and L. Girardin, Phys. Rev. 188, 1517 (1969).

[20]R. G. Korteling and E. K. Hyde, Phys. Rev. 136, B425 (1964).

[21]V. P. Crespo, J. M. Alexander, and E. K. Hyde, Phys. Rev. 131, 1765 (1963).

Differential Cross Sections for Small-Angle Scattering of 24-MeV Neutrons by Protons

T. G. Masterson*

University of Wisconsin, Madison, Wisconsin 53706†

(Received 17 April 1972)

Absolute n-p elastic scattering cross sections were measured at 19.5 and 25.1° (lab) for an incident neutron energy of 24 MeV. A liquid scintillator detected both the incident and scattered neutrons. The scatterer was a liquid scintillator also. The c.m. differential cross sections were 31.3 ± 0.5 and 30.7 ± 0.6 mb/sr at c.m. scattering angles of 39.3 and 50.5°, respectively. The present results agree with the cross sections predicted by Hopkins and Breit.

I. INTRODUCTION

An accurate knowledge of n-p differential cross sections tests our understanding of the nucleon-nucleon interaction and is needed for the measurement of fast-neutron flux. In 1957 Gammel[1] proposed an energy-dependent fit to the available data of the form $A(1 + B\cos^2\Theta_{c.m.})$ for energies below 42 MeV. Later data[2] have shown that the interaction is not symmetric about 90° in the c.m. system indicating the need for a $\cos\Theta$ term. Recently, Hopkins and Breit[3] have used the Yale and Lawrence Radiation Laboratory (LRL) nucleon-nucleon phase-shift analyses to obtain fourth-order Legendre-polynomial expansions for the differential cross section. They predict that the coefficients of the P_1 and P_2 terms have approximately the same magnitude between 20 and 30 MeV. At 24 MeV, the anisotropy in the cross section reaches 10%, and the P_1 and P_2 terms account for most of this anisotropy.

Most measurements of the differential cross section have used a counter telescope for detecting recoil protons, but this method does not work at forward angles because of the small recoil proton energy. The most accurate measurements near 24 MeV are by Rothenberg[4] and Burrows,[5] who has extended the range of this method down to a c.m. scattering angle of about 70°. These measurements are all relative and must be normalized to the total cross section. This normalization requires a knowledge of the scattering at small angles where the cross section is not well known. The only previous forward-angle scattering measurement was by the Harwell group[2] and their energy resolution was poor [full width at half maximum (FWHM) of 5 MeV].

The present paper reports an absolute measurement of the differential scattering cross section at 19.5 and 25.1° (lab). Both the intensity of neutrons scattered through an angle θ by a target scintillator and the intensity of the incident 0° neutron beam [see Figs. 1(a) and 1(b)] were measured. The use of the same detector for both measurements made an absolute determination of the incident flux density unnecessary. Only the relative efficiencies[6] of the detector for neutrons before and after scattering had to be known to normalize the number of neutrons detected at θ to the number incident on the target. The present

data provide measurements of the differential cross section at 39.3 and 50.5° (c.m.). These results may be combined with the relative measurements in the backward hemisphere (such as those by Rothenberg[4] and Burrows[5]) and with the well-known total cross section to give an angular distribution.

II. EXPERIMENTAL METHOD

A. General

Neutrons of 24-MeV lab energy were incident on a target scintillator. The neutrons scattered through an angle θ pass into a detecting scintillator. The target was a liquid hydrocarbon scintillator, so that the background could be reduced by requiring fast coincidences between the recoil protons of the target and the detector scintillators. The 0° neutron flux density was also measured with the detector. The count rate of neutrons observed at 0° depends on the incident flux and the detector efficiency for 24-MeV neutrons. The count rate of neutrons observed at the lab scattering angle θ depends on the same incident flux, the n-p differential cross section, and the efficiency of the detector for neutrons of energy $E_0 \cos^2\theta$. The ratio of these two count rates gives the differential cross section and is independent of the value of the incident neutron flux. The resulting cross section depends only on the ratio of the detector efficiencies at two nearby energies.

B. Neutron Source

The neutron source was the reaction $T(d, n)^4$He. Deuterons of 7.0-MeV energy from a tandem accelerator were incident on a tritium gas cell. Figure 1(c) shows an expanded view of the tritium cell. The cell was 3.8 cm long and contained about 20 Ci of tritium when filled to 1 atm. Gas pressures ranged from 0.8 to 1.8 atm. Entrance and exit foils were 2.5-μm molybdenum and were changed every other day on the accelerator. Beam collimators prevented deuterons from hitting the tantalum washers which supported the molybdenum foils. The cell had an evacuated backstop and was air-cooled to minimize beam heating effects. This design insured that the neutron flux density was the same for all runs. Had the deuteron beam stopped in the tritium cell, heating effects would have changed the local tritium pressure and consequently the neutron source strength. The backstop was larger in diameter than the gas cell to prevent attenuation of the neutron beam by the walls of the backstop in the ±3° range about the 0° direction. A 0.5-mm gold foil stopped the deuteron beam. It was replaced periodically to reduce the number of neutrons produced by the reaction $D(d, n)^3$He.

The mean deuteron energy at the center of the tritium cell was 6.84 MeV (for ~1 atm T_2 pressure). This resulted in approximately 1.6×10^7 neutrons sr^{-1} μC^{-1} at 0° with an energy of 24.03 ± 0.08 MeV.
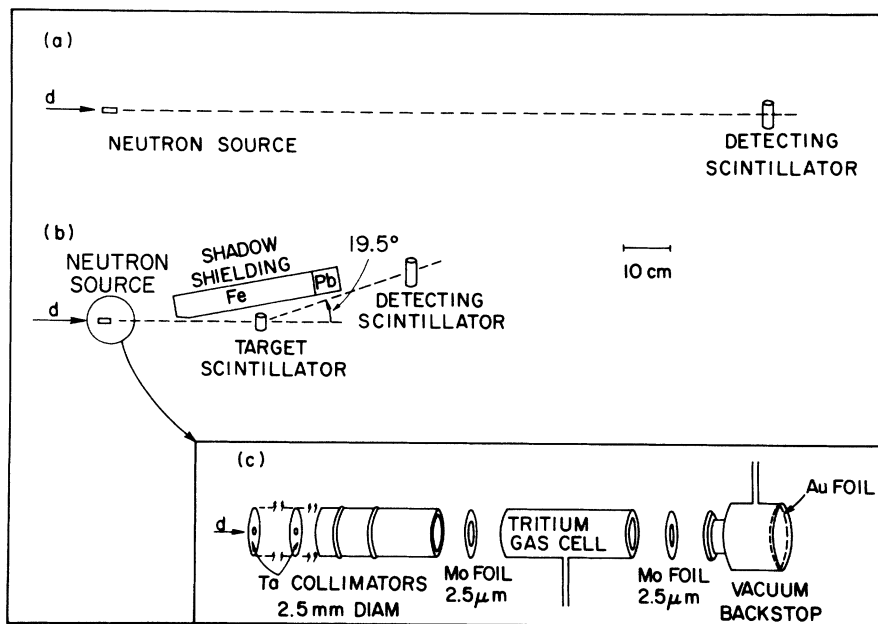

FIG. 1. (a) Geometry for 0° flux measurement, (b) scattering geometry, and (c) detail of tritium gas cell.

C. Apparatus

Figures 1(a) and 1(b) show the apparatus and geometry used. The scattering target and the detector were scintillators mounted on RCA 8575 and Amperex XP1021 photomultiplier tubes, respectively. They were mounted to allow adjustment in the plane perpendicular to the beam.

Both target and detector had Lucite caps with a 0.4-mm-diam rod sticking up through the center. This rod defined the center of each scintillator. Distances between the scintillators and gas cell were measured to ±0.2 mm. The target was a 2.5-cm-diam×2.5-cm-high NE 218 liquid scintillator[7] in a glass cylinder wrapped in aluminum foil and mounted on an RCA 8575 phototube with its axis perpendicular to the beam direction. The mass[7] of the scintillator liquid was 11.37 g and the H/C ratio[8] was 1.28. The total number of hydrogen atoms in the sample was $(0.659 \pm 0.003) \times 10^{24}$. The detector was a 2.5-cm-diam by 5.1-cm-high NE 218 liquid scintillator.

D. Electronics

(i) *Phototube stabilization.* The count rate in the target scintillator was just under 1 MHz. A Zener diode string and capacitor bank stabilized the voltage at each of the last four dynodes and increased the current handling capacity of the bleeder string. The string was air-cooled and operated at about 5 mA. With the diode string in operation, no change in the pulse-height spectrum of a ^{60}Co source was observed for count rates up to 5 MHz.

(ii) *Electronics for data acquisition.* The electronics provided recoil-proton pulse-height spectra for neutrons scattered from the target scintillator into the detector scintillator. Figure 2(a) is a simplified block diagram of the electronics. Neutrons were detected in both target and detector, and a fast [time-of-flight (TOF)] coincidence requirement reduced background. A pulse-shape-discrimination system rejected γ-ray pulses from the detector. Figure 2(b) is a diagram of the actual electronics used.

E. Procedures for Taking Data

The beam current was usually between 1 and 2 μA, the lower limit determined by count-rate considerations (0.5 counts/sec) and the upper limit by the maximum allowable beam on the molybdenum windows. The maximum safe current for nickel foils[9] was assumed for molybdenum.

The angular distribution of the neutron flux near 0° was measured. It varied by less than 2% over the area of the target scintillator. The data analysis took into account these deviations.

A current integrator measured the charge incident on the tritium gas cell. The calibration and zero point of the current integrator were checked at the beginning of each accelerator running period. The offset current measured with no beam on the target was less than 0.2% of the target current. A correction for this offset current was applied.

Both maximal and minimal (shadow) shielding were tried in an attempt to reduce background. Foreground/background ratios were approximately the same in each case. Observed backgrounds were about 8% at 25.1° and 28% at 19.5°. Shadow shielding was used because it was easily removable for 0° normalization runs. [See steps (1) and (4) below.] The shadow shield consisted of 30-cm iron plus 5-cm lead in the direct path of neutrons from the gas cell to the detector. [See Fig. 1(b).]

The following procedure was used in taking data:

(1) Measurement of 0° neutron flux. A 0° normalization run in the direct neutron beam taken with the detector far enough away (142 cm) from the neutron source that the count rate was less than 1 kHz. The count rate was reduced by moving the detector away from the neutron source rather than by decreasing the beam current so that the neutron source strength would be the same for this run as for each of the following runs (2)–(4). This procedure also eliminated any residual effects due to heating of the tritium cell, since the deuteron current was the same for all runs.

(2) Background measurement. A 41-cm-long iron shadow bar was inserted between the gas cell and the detector for a 0° background run. Typical recoil-proton spectra from steps (1) and (2) are shown in Fig. 3(a).

(3) Scattering data. The detector was positioned at the scattering angle θ, and the target scintillator was raised into the direct neutron beam. A TOF coincidence requirement between target and detecting scintillators was imposed, and data were collected for about 1 h (5000 μC). A TOF spectrum of particles scattered by the target scintillator and observed in the detecting scintillator is shown in Fig. 4. These particles satisfy a fast-coincidence requirement and the requirement that the particle seen in the detecting scintillator be a neutron. A "real" neutron is a neutron which satisfies these requirements. One channel of the TOF spectrum of "real" neutrons is approximately 0.2 nsec and the FWHM of the timing spectrum is about 2 nsec. A simultaneously measured "accidental" TOF spectrum is also shown on the same figure. "Accidental" means that the particle seen in the detecting scintillator was a neutron which did not meet the flight-time

requirements. The "accidental" spectrum was obtained by delaying one side of the coincidence system by about 15 nsec. This delay has been removed in the figure for comparison purposes. The effect of the slight differences in the length of time for which the real and accidental coincidence gates were open was included in the data analysis.

A typical "real" recoil-proton spectrum observed at a scattering angle of 25.1° is shown in Fig. 3(b). This spectrum shows the pulse-height distribution of recoil protons produced by "real" neutrons and is gated by the same logic as the "real" TOF spectrum as indicated by the electronics shown in Fig. 2(b). The numbers above the arrows indicate the bias energy expressed as a fraction of the incident neutron energy. The location of the arrows takes into account the non-linear response of the scintillator which was measured in a separate experiment.[6] An "accidental" spectrum was measured simultaneously. It was gated by the same logic as the "accidental" TOF spectrum. Figure 3(c) shows spectra obtained at a scattering angle of 19.5°. Since the background is 3 times higher here, the present method has limited usefulness at smaller angles.

FIG. 2. (a) Simplified block diagram of electronics; (b) electronics used in data collection: 1: recoil proton spectra gated by "real" neutrons 3 or "accidental" neutrons 5, 2: TAC spectra gated by "real" neutrons 4 or "accidental" neutrons 6, 7: fast linear spectrum from target scintillator gated by TOF and n-γ requirements, 8: n-γ spectrum. The abbreviations used are ADC: analog-to-digital converter, DDL: double delay line, SCA: single-channel analyzer, TAC: time-to-amplitude converter.

(4) Scattering data background. An iron shadow bar was inserted between target and detector (the shadow shielding between gas cell and detector remained in place) for a background run. All shielding was then removed, the target scintillator was lowered out of the 0° neutron beam, and the detecting scintillator was moved to its 0° location for another 0° flux measurement.
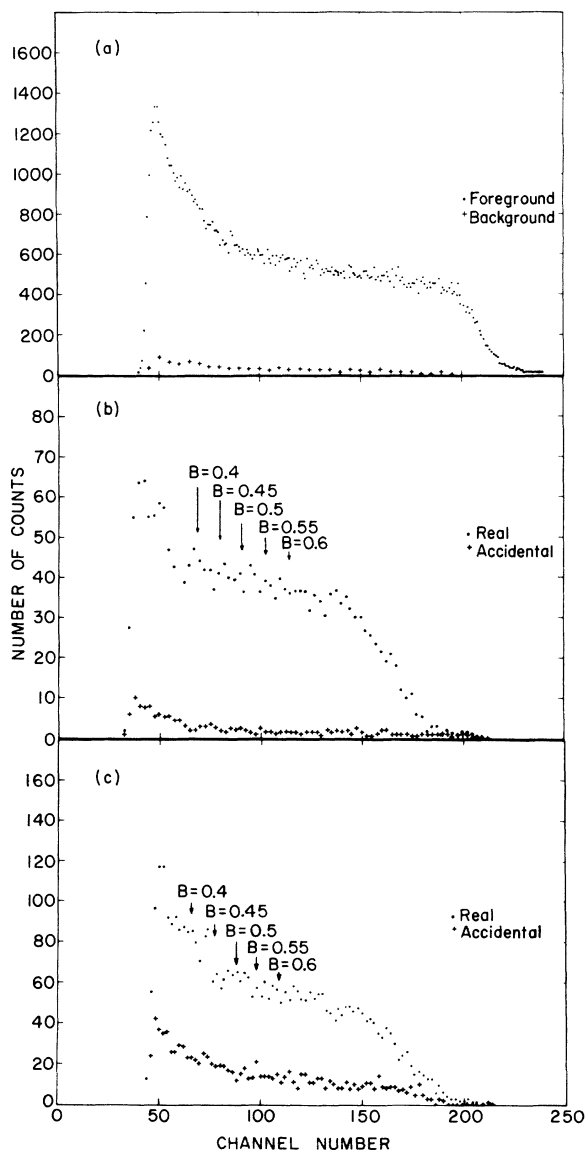

FIG. 3. (a) Recoil-proton spectra observed in the 0° neutron beam. (b) Recoil-proton spectrum observed at a scattering angle of 25.1°. The numbers above the arrows indicate biases expressed as a fraction of the incident neutron energy. Their value includes the effect of the nonlinear response of the scintillator. (c) Recoil-proton spectrum observed at a scattering angle of 19.5°.

III. THEORY AND ANALYSIS

The differential cross section for neutrons scattered by protons through a lab angle θ is[10]

$$\sigma(\theta) = \frac{s^2 d^2}{d_0^2} \frac{f_B(E_0)}{f_B(E_1)} \frac{\sigma_{np}(E_0)}{\sigma_{np}(E_1)} \frac{1}{n_p} \frac{A_\theta}{B_0}, \qquad (1)$$

where s is the distance from neutron source to target scintillator, d is the distance from target scintillator to detecting scintillator, d_0 is the distance from neutron source to detecting scintillator for 0° measurements, $\sigma_{np}(E)$ is the n-p total cross section at energy E, n_p is the total number of protons in the target, A_θ is the number of neutrons detected per unit charge after being scattered from the target into the detector, B_0 is the number of neutrons detected per unit charge in the 0° position, and f_B is the fraction of the total number of recoil protons detected at a given bias. The bias factor f_B is given by

$$f_B = \int_{\Psi_{\min}}^{\pi} \sigma_{c.m.}(\Psi)(\sin\Psi)d\Psi \Big/ \int_0^{\pi} \sigma_{c.m.}(\Psi)(\sin\Psi)d\Psi, \qquad (2)$$

where Ψ is the c.m. scattering angle and $\Psi_{\min}$ is the neutron scattering angle at which the recoil-proton energy is equal to the bias energy B. The c.m. differential cross section is $\sigma_{c.m.}(\Psi)$ and the integral is over a differential volume element inside the detector. Table I gives values of the ratio $f_B(E_0)/f_B(E_1)$ as a function of bias energy for various assumed angular distributions. The table indicates that for these angles and biases the assumed angular distribution has little effect on the determination of the differential cross section. The Hopkins and Breit angular distribution derived from the Yale phase shifts was used in this calculation. The lab cross sections were converted to the c.m. system using the relativistic kinematics

TABLE I. Effect of different angular distributions on bias factors.

Bias (B/E_0)	Ratio of bias factors $f_B(E_0)/f_B(E_1)$ for angular distributions		
	Isotropic	Gammel	Hopkins
$E_0 = 24$ MeV, $E_1 = 21.35$ MeV			
0.45	1.113	1.110	1.115
0.5	1.142	1.137	1.146
0.55	1.179	1.172	1.186
$E_0 = 24$ MeV, $E_1 = 19.69$ MeV			
0.45	1.219	1.208	1.217
0.5	1.281	1.265	1.282
0.55	1.366	1.345	1.372

program RELKIN.[11] Not yet included in the relation (1) are the effects of multiple scattering, exponential attenuation, and wall effects. These will be discussed in Sec. IV.

A computer program was used to analyze all recoil-proton pulse-height spectra and to calculate a laboratory differential cross section. It took into account backgrounds, accidental coincidences, bias effects, and the nonlinear response of the scintillator. It also included the effects of transmissions through shadow bars, differences in widths of time-to-amplitude converter (TAC) spectra, dead time, analog-to-digital converter (ADC), and current-integrator corrections. In addition, the program was used to calculate statistical errors.

IV. CORRECTIONS

A. Multiple Scattering

Consider neutrons which have scattered once from a hydrogen atom in the target scintillator through an angle θ towards the detector. The number of neutrons going in this direction may be decreased by collisions with either hydrogen or carbon atoms in their paths while leaving the target scintillator. This is called exponential attenuation of the outgoing beam or out scattering. The number of neutrons headed towards the detector may be increased by neutrons which have scattered previously from hydrogen atoms in a direction away from the detector and then scatter from either H or C towards the detector. The scattered flux may also be increased by neutrons which have scattered previously from carbon in any direction and then from hydrogen towards the detector. Neutrons interacting only with carbon are not included because carbon recoils are not detected in the target scintillator, since the bias level on the target scintillator was set above the maximum light output for both carbon recoils and α particles from reactions in carbon.

A Monte Carlo computer program was used to trace the trajectories of about 6×10^5 interacting neutrons through the target scintillator and to calculate the numbers of all possible in scattering and out scattering collisions. At 25.1°, 5.5% of the detected particles were due to in scattering, while 9.0% had been out scattered for a net correction of +3.4%. At 19.5°, in scattering was 2.8%, out scattering was 8.7% and the correction to the scattered flux was +5.8%.

B. Finite Geometry

The tritium gas cell is actually a neutron source of finite length and not a point source. Neutrons are assumed to be produced uniformly over this length. Thus the front of this cell subtends a different solid angle at the target than the back of the cell. The average count rate $\bar{A}_\theta$ may be written as[10]

$$\bar{A}_\theta = A_\theta \frac{1}{1 - (L/2s)^2} ,$$

where L is the length of the tritium gas cell and s is the distance from the center of the gas cell to the center of the target. For $L = 3.8$ cm and $s = 34.5$ cm this represents a correction of -0.3% to the differential cross section. This correction is negligible when the detector is at 0°, since the distance to the detector is about 142 cm.

The same correction may also be made for the finite length of the target. Here the differential cross section must be multiplied by the factor $1 - (D/2d)^2 = 0.999$ (where the target diameter D is 2.54 cm and d is 33.4 cm) for a correction of -0.1%.

C. Attenuation in Detector

The flux actually measured in the detecting scintillator is not uniform throughout the scintillator, but is exponentially attenuated along its path through the scintillator by collisions of the neutrons with C and H nuclei. By performing an integration over the volume of the scintillator[10] we find, for an incident energy of 24 MeV, 92.3% of the incident neutrons are transmitted through the scintillator. At a scattering angle of 19.5°, 91.8% of the scattered neutron beam is transmitted through the detecting scintillator. At 25°, 91.1% goes through. Since the attenuation depends on the energy of the neutrons incident on the detecting scintillator, corrections to the differential cross section of 0.5% at 19.5° and 1.3% at 25° result.

D. Attenuation in Target and Air

The actual neutron flux in the detecting scintillator differed from that measured at 0° because of the exponential attenuation of the neutron beam as it passed through the target. Five separate factors must be taken into account in the calculation of this effect:

(1) The exponential attenuation of the neutron beam entering the target scintillator must be included. This will decrease the average beam intensity passing through the target. This correction was calculated by partitioning the target scintillator into 15 segments and calculating the transmission (T_i) through half the thickness of each segment.

(2) The effect of exponential attenuation of the neutron beam coming out of the target towards the detector must be included. Here we must con-

sider both the decrease in the flux density directed towards the detector by outscattering and the increase in this flux density by neutrons which scatter first in some other direction and then towards the detector (in scattering). This calculation has been done more accurately in the multiple-scattering program but is included here because it is also needed in the calculation of the average scattering angle.

(3) The effect of exponential attenuation by the material (glass, tape, and aluminum foil) surrounding the scintillator fluid must also be included. This must be considered for both incident and outgoing neutron beams. This correction was calculated from the experimentally observed transmission through the scintillator (including container, etc.) and the calculated transmission through the scintillator fluid alone. This was a 3.9% correction to the differential cross section.

(4) The effect of differing distances and scattering angles at different locations in the target scintillator must also be included.

(5) Exponential attenuation by the air must be taken into account. This applies to both the 0° measurement of the direct flux density and the measurement of the scattered flux density. The effect will be greater at 0° than at the scattering angle θ, since the distance from the neutron source to the detector is greater at 0°. The net correction to the cross section is −0.1%.

The target scintillator was partitioned into 15 segments (5 in the horizontal plane by 3 in the vertical plane) to calculate and measure the effects (1), (2), and (4) above.

The differential cross section [Eq. (1)] may be rewritten as[10]

$$\bar{\sigma}(\bar{\theta}) = (1 + \delta)\sigma(\theta),\qquad(3)$$

where

$$1 + \delta = \left[\sum_{i=1}^{15}\frac{C_i}{C_8}\,T_i T_i'\,\frac{V_i}{V}\left(\frac{d_8}{d_i}\right)^2\right]^{-1}.\qquad(4)$$

C_i is the measured neutron flux in the ith segment (8 denotes the middle position, the position at which all 0° flux measurements were made). T_i is the transmission of the incoming neutron beam through half the thickness of the ith segment of the scintillator fluid. T_i' is the transmission of the outgoing neutron beam through the remaining thickness of scintillator fluid towards the target. T_i' was set equal to 1 to calculate δ because this effect is already included in the multiple-scattering correction. It was needed for the average scattering angle calculation. V_i is the volume of the ith segment, V is the total volume, and d_i is the distance from the center of the ith segment to the detecting scintillator. At a scattering

angle of 19.5°, δ is 0.077; at 25.1°, δ is 0.076.

Average scattering angles were calculated from these parameters using the equation

$$\bar{\theta} = \sum_{i=1}^{15}\theta_i V_i\frac{C_i}{C_8}\frac{1}{d_i^2}T_i T_i'\Big/\sum_{i=1}^{15}V_i\frac{C_i}{C_8}\frac{1}{d_i^2}T_i T_i'.\qquad(5)$$

A geometrical θ of 19.46° corresponded to $\bar{\theta}$ = 19.53°, and a geometrical θ of 25.09° became 25.13°.

E. Wall Effects

The range of a 24-MeV proton recoiling from a head-on collision with a 24-MeV neutron is 0.67 cm in toluene, the liquid of the scintillator. The diameter of the scintillator is 2.54 cm. Consequently, many of the recoils in the detector do not have their full range inside the scintillator, and their observed light output corresponds to an energy less than their actual energy.

A Monte Carlo routine was used to calculate this effect. The program traced the paths of some 2×10^5 neutrons of each incident energy through the scintillator. All incident neutrons interacted with the scintillator and appropriately weighted random numbers were chosen for all scattering parameters.

Since this wall effect occurs both when the detector is at 0° for an incident flux density measurement and at the scattering angle θ, the ratio of the effects in both places will give the correction to the differential cross section. At a bias of $0.5E_0$, the correction to the differential cross section is −2% at 19.5° and −3.3% at 25.1°.
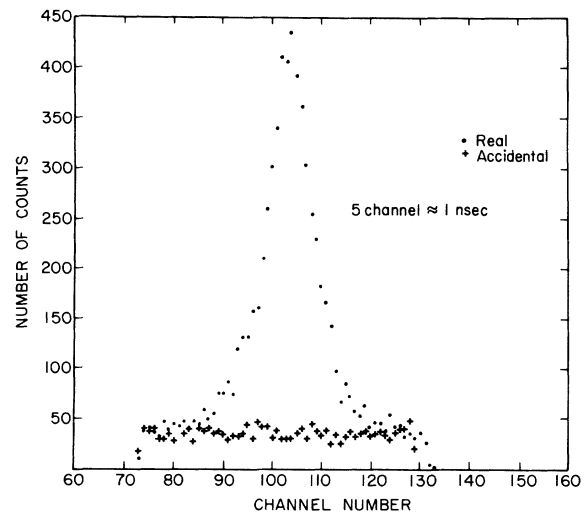

FIG. 4. Time-of-flight spectra for neutrons scattered from the target scintillator into the detecting scintillator. FWHM is approximately 2 nsec.

Wall effects in the target scintillator must also be included. If a neutron is to meet all the electronic requirements for scattering from a proton in the target into the detecting scintillator, it must produce a detectable recoil proton in the target scintillator. A lower level discriminator threshold was set on pulses coming from the target scintillator. If a recoil proton is produced so close to the wall of the target scintillator that part of its range lies outside the scintillator, this recoil will be lost if the observed pulse height is less than the discriminator threshold. This wall effect is simple to calculate because the geometry involved is well determined. In order for the scattered neutron to hit the detecting scintillator the scattering must take place in or near the horizontal plane and all recoils must go in approximately the same direction. Let the minimum detectable path length be ϵ. The number of recoils which are not detected because they occur too close to the wall is then proportional to the nonoverlapping area of two circles with their centers separated by a distance ϵ. The fraction of recoils occurring in this area is given by[10]

$$f_m = 1 - \frac{2}{\pi}\cos^{-1}\left(\frac{\epsilon}{2r}\right) + \frac{\epsilon}{\pi r}\left(1 - \frac{\epsilon^2}{4r^2}\right)^{1/2}, \qquad (6)$$

where r is the scintillator radius. The calculation is exact for any value of ϵ.

At 19.5°, the minimum detectable recoil energy was 1.4 MeV. This corresponds to an ϵ of 0.0046 cm (from Janni[12]) and a correction to the differential cross section of +0.2%. At 25°, the minimum detectable recoil energy was 2.25 MeV corresponding to an ϵ of 0.010 cm and a correction to the differential cross section of +0.5%.

V. RESULTS

A. Measured Cross Sections

Table II presents the measured differential cross sections at an average scattering angle of 25.1°(lab) as a function of bias energy. The values quoted are in the lab and uncorrected. Corrections are given in Sec. V B. The errors given in this table are statistical only. Data Sets I–III differ in the tritium pressure of gas cell used for the neutron source. The over-all average is weighted by the statistical error of each data set. Lower bias levels are excluded because the reactions $D(d, n)^3He$ and $^{12}C(n, n')3\alpha$ enter.

Figure 5(a) is a histogram of all the differential cross-section measurements at 25°. Each square represents a measurement of the differential
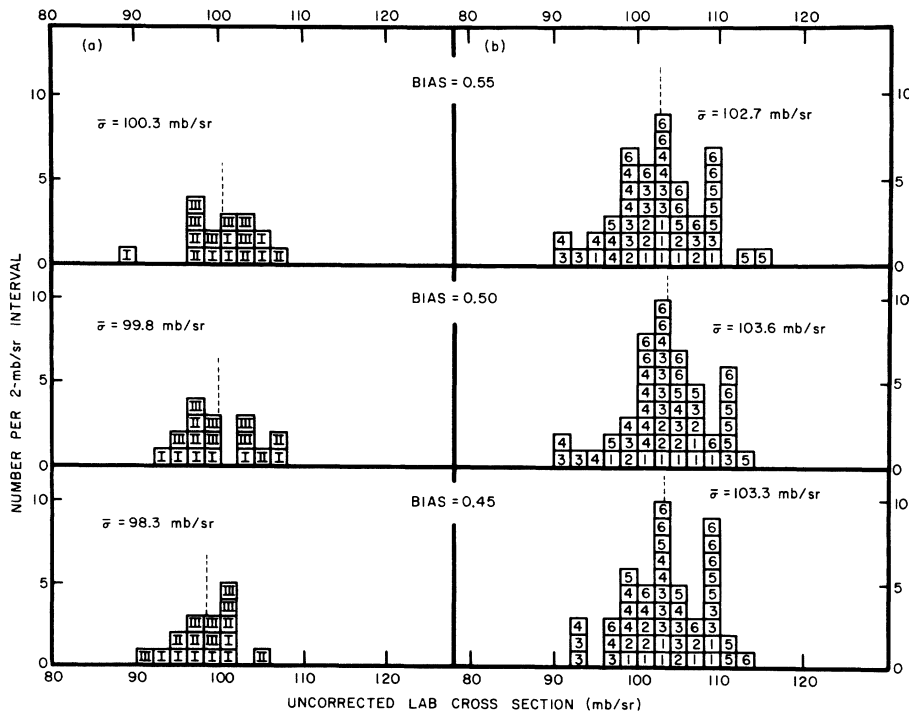

FIG. 5. (a) Histogram of 25.1° data as a function of bias energy. (b) Histogram of 19.5° data as a function of bias energy. Each block represents a differential cross-section measurement within the indicated 2-mb/sr interval.

cross section within the indicated 2-mb/sr inter-
val. Statistical errors on each point are about 5%.
The spread in the data points about the average
values (indicated on the histograms by the dashed
lines) was used to obtain standard errors.

Table III presents the measured differential
cross sections at an average lab scattering angle
of 19.5°. The cross-section values are in the lab
system and uncorrected, and the errors quoted
in this table are statistical only. Data Sets 1-6
differ in the electronics used and in the tritium
pressure in the neutron source.

Figure 5(b) is a histogram of the differential
cross-section measurements at 19.5° as a func-
tion of bias energy. Statistical errors on each
point are approximately 5%. No distinction is
made between data from neutrons scattered to the
left and to the right in the lab in these histograms,
because no statistically significant differences
were found between left and right scattering. The
dashed lines again indicate the average values,
and the spread in the data about this value was
used to obtain a standard error.

B. Corrections to the Cross-Section Data

Table IV presents the corrections to the data.
The uncertainty in the differential cross section
due to these corrections is approximately 1.5%,
and is principally due to uncertainties in the ex-
ponential attenuation correction δ, the multiple-
scattering correction, and uncertainties in the
differential cross section itself which results in
errors in the bias factor f_B (see below).

Table V presents the corrected c.m. cross sec-
tions and the corrected c.m. angles at which they
were observed. The average values are obtained
by averaging data over all biases. Since the data
sets are correlated, this averaging does not im-
prove the statistical accuracy.

C. Error Analysis

Table VI lists the errors in the cross-section
measurement. The standard error was estimated
by taking sums of squares of deviations from the
mean cross section at each bias energy and divid-
ing by $N(N-1)$, where N is the number of obser-
vations. 16 separate measurements were made
of the differential cross section at 25°, 50 at 19.5°.

The error in δ was estimated by observing the
changes that occurred in the calculated value of δ
with extreme variation of the input parameters.
It includes errors for target exponential attenua-
tion corrections. The error in f_B was estimated
by assuming that the bias was known to 1% and
calculating the uncertainty in f_B as a function of
the scattering angle θ. This corresponds to an
uncertainty of approximately 4 channels in the
estimate of the maximum recoil-proton energy
in the direct neutron beam. The error in n_p is the
error quoted by Galbraith Laboratories in their
analysis of the hydrogen and carbon content of the
scintillator fluid. The error in the correction
for the finite range of the recoil protons is the
statistical error based on the number of neutron
trajectories traced by the Monte Carlo calcula-
tion. The multiple-scattering error is the statis-
tical error based on the number of neutron tra-
jectories followed by the Monte Carlo multiple-
scattering program. The column labeled "rms
error" is the rms sum of all the errors quoted
in the table except those due to counting statistics.
The final column is the rms sum of all errors.

VI. CONCLUSIONS

The cross section measured at 19.5° (lab) or
39.3° (c.m.) is 31.3 ± 0.5 mb/sr. The cross sec-
tion calculated from the LRL phase shifts by
Hopkins and Breit[3] is 31.3 mb/sr. The value they

TABLE II. Laboratory differential cross sections
measured at 25.1°. No corrections are included in these
values other than those contained in the data-analysis
program.

Data set	Bias = 0.45 σ (mb/sr)	Δσ (%)	Bias = 0.5 σ (mb/sr)	Δσ (%)	Bias = 0.55 σ (mb/sr)	Δσ (%)
I	98.2	1.9	99.4	2.1	100.4	2.2
II	98.4	1.7	100.4	2.0	100.4	2.2
III	98.4	1.6	99.7	1.7	100.1	1.9
Average	98.3	1.0	99.8	1.1	100.3	1.2

TABLE III. Laboratory differential cross sections
measured at 19.5°. No corrections are included in these
values other than those contained in the data-analysis
program.

Data set	Bias = 0.45 σ (mb/sr)	Δσ (%)	Bias = 0.50 σ (mb/sr)	Δσ (%)	Bias = 0.55 σ (mb/sr)	Δσ (%)
1	102.8	1.3	103.0	1.4	101.9	1.5
2	103.2	1.6	103.8	1.7	103.4	1.9
3	102.3	1.3	102.2	1.4	101.1	1.5
4	100.1	1.3	100.0	1.4	98.2	1.6
5	106.7	1.6	108.7	1.7	109.0	1.8
6	106.0	1.4	105.6	1.5	104.7	1.6
Average	103.3	0.6	103.6	0.6	102.7	0.7

TABLE IV. Corrections. All corrections are given in %.

θ_{lab} (deg)	Bias B/E_0	Attenuation Ref. a	Ref. b	Ref. c	Ref. d	Ref. e	Ref. f	Ref. g	Ref. h	Ref. i	Total
19.5	0.45	7.7	3.9	−0.1	−0.3	−0.1	5.8	0.5	0.2	−1.8	15.7
	0.50									−2.0	15.5
	0.55									−2.3	15.3
25.1	0.45	7.6	3.9	−0.1	−0.3	−0.1	3.4	1.3	0.5	−2.9	13.3
	0.50									−3.3	12.9
	0.55									−3.7	12.5

[a] Exponential attenuation of the neutron beam by the target scintillator fluid.

[b] Exponential attenuation of the neutron beam by the container of the target scintillator fluid.

[c] Exponential attenuation of the neutron beam by air.

[d] Effect of finite length of neutron source.

[e] Effect of finite length of target.

[f] Multiple-scattering correction.

[g] Effect of finite detector thickness − exponential attenuation of neutron beam in detector.

[h] Effect of finite range of recoil protons in target.

[i] Effect of finite range of recoil protons in detector.

TABLE V. Summary of cross-section measurements and corrections. $\bar{\sigma}(39.3°) = 31.3 \pm 0.5$ mb/sr, $\bar{\sigma}(50.5°) = 7 \pm 0.6$ mb/sr.

θ_{lab}	Bias (B/E_0)	σ_{lab} uncorrected (mb/sr)	Correction (%)	c.m. conversion factor	$\theta_{c.m.}$ (mb/sr)	$\theta_{c.m.}$
19.5°	0.45	103.3	15.7	0.262	31.4	39.3°
	0.50	103.6	15.5	0.262	31.4	39.3°
	0.55	102.7	15.3	0.262	31.1	39.3°
25.1°	0.45	98.3	13.3	0.273	30.5	50.5°
	0.50	99.8	12.9	0.273	30.8	50.5°
	0.55	100.3	12.5	0.273	30.8	50.5°

TABLE VI. Errors. All values are given in %.

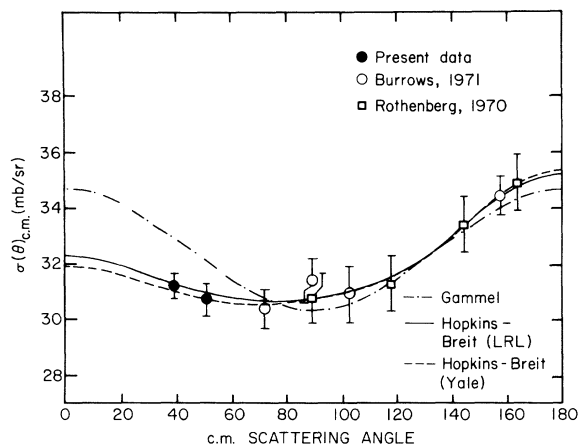| θ (lab)	Bias (B/E_0)	Counting statistics	Standard error	δ	f_B	n_p	Finite range of recoil protons	Multiple scattering	rms error without counting statistics	Over-all error
19.5°	0.45	0.6	0.7	0.5	0.7	0.4	0.2	0.6	1.3	1.4
	0.50	0.6	0.7	0.5	0.7	0.4	0.2	0.6	1.3	1.4
	0.55	0.7	0.7	0.5	0.7	0.4	0.2	0.6	1.3	1.5
25.1°	0.45	1.0	1.0	0.6	1.1	0.4	0.3	0.6	1.7	2.0
	0.50	1.1	1.1	0.6	1.1	0.4	0.3	0.6	1.8	2.1
	0.55	1.2	1.1	0.6	1.1	0.4	0.3	0.6	1.8	2.2

FIG. 6. Wisconsin n-p differential cross-section measurements. Only the present results are absolute determinations.

calculate from the Yale phase shifts is 31.0 mb/sr.

The cross section measured at 25.1° (lab) or 50.5° (c.m.) is 30.7 ± 0.6 mb/sr. The cross section calculated from the LRL phase shifts by Hop-

kins and Breit is 31.0 mb/sr. The value they calculate from the Yale phase shifts is 30.7 mb/sr.

Figure 6 is a plot of all the available 24-MeV data.[4,5] All measurements were carried out at Wisconsin using two different experimental techniques. Also plotted on the graph for comparison are a symmetric Gammel curve, and both the LRL and Yale phase-shift calculations from Hopkins and Breit. No attempt has been made here to make an additional fit to the data. The data confirm the expected fore-aft asymmetry and indicate that the Hopkins and Breit predictions are impressively good.

ACKNOWLEDGMENTS

---

[1]J. L. Gammel, in *Fast Neutron Physics, Part II*, edited by J. B. Marion and J. L. Fowler (Interscience, New York, 1963), p. 2185.

[2]J. P. Scanlon, G. H. Stafford, J. J. Thresher, P. H. Bowen, and A. Langsford, Nucl. Phys. 41, 401 (1963).

[3]J. C. Hopkins and G. Breit, Nucl. Data A9, 137 (1971).

[4]L. N. Rothenberg, Phys. Rev. C 1, 1226 (1970).

[5]T. W. Burrows, Bull. Am. Phys. Soc. 17, 151 (1972), and Ph.D. thesis, University of Wisconsin, 1972 (unpublished).

[6]T. G. Masterson, Nucl. Instr. Methods 88, 61 (1970).

[7]Supplied by Nuclear Enterprises, Inc., San Carlos, Calif. The mass of the target scintillator fluid was also measured by this firm.

[8]Determined by Galbraith Laboratories, Knoxville, Tenn.

[9]J. B. Marion and F. C. Young, *Nuclear Reaction Analysis* (North-Holland, Amsterdam. 1968), p. 116.

[10]T. G. Masterson, Ph.D. thesis, University of Wisconsin, 1971 (unpublished).

[11]R. E. Phillips and S. T. Thornton, ORNL Report No. 4179, 1967 (unpublished).

[12]J. F. Janni, Technical Report No. AFWL-TR-65-150, 1966 (unpublished).